Molecular Crystals and Liquid Crystals Science and Technology. Section A. Molecular Crystals and Liquid Crystals

Publication details, including instructions for authors and subscription information:
http://www.tandfonline.com/loi/gmcl19

Configuration Transitions of Nematic Droplets in PDLC

Zhou Fu-shan [a b], Ou-Yang Zhong-can [a b], Xu Shou-yi [a], Gao Hong-jing [a], Zhang Bai-zhe [a] & You Shi-ji [a]

[a] Beijing Engineering Research Center of Liquid Crystal Technology, Tsinghua University, Department of Chemistry, Beijing, 100084, China

[b] Institute of Theoretical Physics, Academia Sinica, P.O.Box 2735, Beijing, 100080, China

Version of record first published: 04 Oct 2006

To cite this article: Zhou Fu-shan, Ou-Yang Zhong-can, Xu Shou-yi, Gao Hong-jing, Zhang Bai-zhe & You Shi-ji (1997): Configuration Transitions of Nematic Droplets in PDLC, Molecular Crystals and Liquid Crystals Science and Technology. Section A. Molecular Crystals and Liquid Crystals, 304:1, 47-58

To link to this article: http://dx.doi.org/10.1080/10587259708046942

Mol. Cryst. Liq. Cryst., 1997, Vol. 304, pp. 47–58
Reprints available directly from the publisher
Photocopying permitted by license only

Configuration transitions of nematic droplets in PDLC

Zhou Fu-shan[1,2], Ou-Yang Zhong-can[1,2], Xu Shou-yi[1],
Gao Hong-jing[1], Zhang Bai-zhe[1], You Shi-ji[1]

[1]Beijing Engineering Research Center of Liquid Crystal Technology,
Department of Chemistry, Tsinghua University, Beijing 100084, China

[2]Institute of Theoretical Physics, Academia Sinica, P.O.Box 2735,
Beijing 100080, China

Received:

Abstract

A general equilibrium equation, including the saddle-splay elastic constant K_{24}, of director configurations of nematic droplets in PDLC with weak homeotropic anchoring is obtained. Numerical simulation shows that: 1) A transition from the axial structure to the bipolar structure occurs at certain threshold value of the ratio of the anchoring strength σ and the electric field strength ξ; 2) A nearly homogeneous orientation of the directors occurs when $\frac{\sigma}{\xi}$ decreases to a certain value; 3) Increasing $\frac{\sigma}{\xi}$ can induce a transition from the radial structure to the axial structure; 4) K_{24} is insensitive to both the radial structure and the axial structure. Optical patterns of droplets with different configurations viewed under polarized optical microscope were also simulated. The numerical method used in the present work is different from that used in previous works and maybe useful in case of more complex boundary conditions.

PACS numbers: 64.70.Md, 61.30.Gd

I Introduction

Recently keen interests have been focused on the behavior of liquid crystals in confined geometry [1-3], in particular, of nematic droplets confined in spherical geometry as in PDLC (polymer dispersed liquid crystals) [4-5]. In such cases, the surface effect and the bulk effect are comparable. Many structures, such as the radial structure , the bipolar structure and the axial structure have been discovered [2, 6-8]. Surface induced phenomena near N-I transitions have also been investigated [9-11]. However, An integrated picture of droplet structure under different conditions is still lacking. In this article we are trying to do some work on this line by considering nematic droplets with weak homeotropic anchoring in an electric field and taking the surface anchoring and the saddle-splay elasticity into consideration.

II Free energy and equilibrium equations

The total free energy of a spherical nematic droplet of constant volume at constant temperature is:

$$\begin{aligned} E_{free}(\mathbf{r}) &= \frac{1}{2}\int_v [K_1(\nabla\cdot\mathbf{n})^2 + K_2(\mathbf{n}\cdot\nabla\times\mathbf{n})^2 + K_3(\mathbf{n}\times\nabla\times\mathbf{n})^2 - \epsilon_0\epsilon_a(\mathbf{n}\cdot\mathbf{E})^2]d\mathbf{r} \\ &- \oint_s [\frac{1}{2}W_0(\mathbf{n}\cdot\mathbf{m})^2 + K_{24}\mathbf{m}\cdot(\mathbf{n}\nabla\cdot\mathbf{n} + \mathbf{n}\times\nabla\times\mathbf{n})]ds. \end{aligned} \tag{1}$$

where K_1, K_2 and K_3 are the splay, the twist and the bend constant respectively, ϵ_a is the dielectric anisotropy, W_0 is the strength of the surface anchor energy, $\mathbf{n}$ and $\mathbf{m}$ are the unit director vector and the unit surface normal vector respectively, and K_{24} is the saddle-splay constant. The surface anchor energy is expressed as:

$$-\frac{1}{2}\oint_s W_0(\mathbf{n}\cdot\mathbf{m})^2 ds \tag{2}$$

Introducing two Lagrange multipliers, $\lambda(\mathbf{r})$ for the volume integral, and $\Lambda(\mathbf{r})$ for the surface integral, we write:

$$F = \int_v f_v d\mathbf{r} + \oint_s f_s ds. \tag{3}$$

with

$$\begin{aligned} f_v &= \frac{1}{2}[K_1(\nabla\cdot\mathbf{n})^2 + K_2(\mathbf{n}\cdot\nabla\times\mathbf{n})^2 + K_3(\mathbf{n}\times\nabla\times\mathbf{n})^2] \\ &- \frac{1}{2}\epsilon_0\epsilon_a(\mathbf{n}\cdot\mathbf{E})^2 - \frac{1}{2}\lambda(\mathbf{r})(\mathbf{n}\cdot\mathbf{n} - 1). \end{aligned} \tag{4}$$

$$f_s = -\frac{1}{2}W_0(\mathbf{n}\cdot\mathbf{m})^2 - K_{24}\mathbf{m}\cdot(\mathbf{n}\nabla\cdot\mathbf{n} + \mathbf{n}\times\nabla\times\mathbf{n}) - \frac{1}{2}\Lambda(\mathbf{r})(\mathbf{n}\cdot\mathbf{n}-1). \tag{5}$$

The Euler-Lagrange equations are:

$$\frac{\partial f_v}{\partial n_i} - \frac{\partial}{\partial x_j}\left(\frac{\partial f_v}{\partial n_{i,j}}\right) = 0, \tag{6}$$

$$\frac{\partial f_s}{\partial n_i} - \frac{\partial}{\partial x_j}\left(\frac{\partial f_s}{\partial n_{i,j}}\right) + m_j\frac{\partial f_v}{\partial n_{i,j}} = 0. \tag{7}$$

where m_j is the j-th component of $\mathbf{m}$. A straight-forward calculation leads to:

$$(K_3-K_1)\nabla(\nabla\cdot\mathbf{n}) - K_3\nabla^2\mathbf{n} + (K_2-K_3)[A\nabla\times\mathbf{n} + \nabla\times(A\mathbf{n})] - \epsilon_0\epsilon_a(\mathbf{n}\cdot\mathbf{E})\mathbf{E} = \lambda(\mathbf{r})\mathbf{n}. \tag{8}$$

in the bulk, and

$$\begin{aligned}&(K_1-2K_{24})\mathbf{m}\cdot(\nabla\cdot\mathbf{n}) - W_0(\mathbf{n}\cdot\mathbf{m})\cdot\mathbf{m} + (K_3-K_2)A(\mathbf{m}\times\mathbf{n})\\ -\ &(K_3-2K_{24})\mathbf{m}\times\nabla\times\mathbf{n} + 2K_{24}(\mathbf{m}\cdot\nabla)\mathbf{n} = \Lambda(\mathbf{r})\mathbf{n}\end{aligned} \tag{9}$$

on the surface, where

$$A = \mathbf{n}\cdot(\nabla\times\mathbf{n}). \tag{10}$$

For simplicity, we consider the one constant approximation, i.e., $K_1 = K_2 = K_3 = \mathrm{K}$. Under this condition, Eq. (8) and Eq. (9) become

$$\nabla^2\mathbf{n} + \gamma(\mathbf{n}\cdot\mathbf{E})\mathbf{E} = \lambda'(\mathbf{r})\mathbf{n}. \tag{11}$$

in the bulk, and

$$\tau(\mathbf{m}\cdot(\nabla\cdot\mathbf{n}) - \mathbf{m}\times\nabla\times\mathbf{n}) - \nu(\mathbf{n}\cdot\mathbf{m}) - \mathbf{m}(\mathbf{m}\cdot\nabla)\mathbf{n} = \Lambda'(\mathbf{r})\mathbf{n}. \tag{12}$$

on the surface, here

$$\gamma = \frac{\epsilon_0\epsilon_a}{K}, \tag{13}$$

$$\tau = \frac{K-2K_{24}}{2K}\cdot\frac{K}{K_{24}}, \tag{14}$$

$$\nu = \frac{W_0}{2K}\cdot\frac{K}{K_{24}}. \tag{15}$$

By scaling transformation, one can see that in a large droplet the director configuration is mainly determined by the surface anchoring strength and in a small droplet elastic torsion play the major role.

In numerically simulating the director configuration, Eq. (11) and Eq. (12) must be rewritten into difference equations. We assume that the director configuration has cylindrical symmetry and treat this problem in spherical coordinates

Due to the complexity of the boundary condition, the relaxation method, which is usually used in treating this kind of problems, should be altered. Here a hybrid method which is a combination of the relaxation method and the fractional-step method (or hill-climbing method) proves simple and reliable. that is, we treat the bulk equation with the relaxation method, the boundary equation with the fractional-step method, and combine them into a unified formula for computer simulation.

Let $\rho = \frac{R}{N}$, $h = \frac{\pi}{C}$, where R is the radius of the droplet, N and C are integers, and denote

$$\mathbf{r}_{ijl} = (r, \theta, \phi) = (i\rho, jh, 2lh) \tag{16}$$

for positive integers $i < N + 1$, $l < 2C + 1$, n_k means the k-th component of n.

Let

$$n_{i,j,k,l} = n_k(\mathbf{r}_{ijl}). \tag{17}$$

Due to the cylindrical symmetry, we simplify $n_{i,j,k,l}$ by $n_{i,j,k}$, that is:

$$n_{i,j,k} = n_{i,j,k,l} \tag{18}$$

After some numerical manipulations, the following formula can be deduced, and is used in iterating in computer simulation:

$$d_{i,j,k} = f(i,j,k) + \delta_{iN} g(i,j,k), \tag{19}$$

$$n_{i,j,k} = \frac{d_{i,j,k}}{|\mathbf{d}_{i,j}|}, \tag{20}$$

where $\mathbf{d}_{i,j}$ is a vector, and

$$\begin{aligned} f(i,j,k) = {} & \frac{1}{a - b\cos^2(jh)}[(i^2 + 2i)n_{i+1,j,k} + \frac{1}{h^2} + \frac{1}{h}cot(jh)n_{i,j+1,k} + i^2 n_{i-1,j,k} + \frac{1}{h^2}n_{i,j-1,k} \\ & - b\delta_{1k}n_{i,j,2}sin(jh)cos(jh) - b\delta_{2k}n_{i,j,1}sin(jh)cos(jh)] \end{aligned} \tag{21}$$

$$g(i,j,k) = n_{i,j,k} - t\{\delta_{1k}\{\tau[2n_{N,j,1} + N(n_{N,j,1} - n_{N-1,j,1}) + cot(jh)n_{N,j,2}$$

$$+ \quad \frac{1}{h}(n_{N,j+1,2} - n_{N,j,2})] - \nu R n_{N,j,1} + N(n_{N,j,1} - n_{N-1,j,1})\}$$
$$+ \quad \delta_{2k}\{\tau[n_{N,j,2} + N(n_{N,j,2} - n_{N-1,j,2}) - \frac{1}{h}(n_{N,j+1,1} - n_{N,j,1})] + N(n_{N,j,2} - n_{N-1,j,2})\}$$
$$+ \quad \delta_{3k}\{\tau n_{N,j,3} + N(\tau+1)(n_{N,j,3} - n_{N-1,j,3})\}\}, \tag{22}$$

$$a = \frac{2}{h^2} + \frac{1}{h}cot(jh) + 2i^2 + 2i, \tag{23}$$
$$\mu = \gamma R^2 E^2, \tag{24}$$
$$b = \mu\frac{i^2}{N^2}. \tag{25}$$

Here $t > 0$.

IV Results

We limit our discussion to cases without twist deformations, and introduce two parameters:

$$\xi = \sqrt{\mu}, \tag{26}$$
$$\sigma = \nu R. \tag{27}$$

The droplet structure can be characterized by two parameters: the anchoring strength σ and the electric field strength μ. We also assume that $K_{24} = K$ (a good approximation to most liquid crystal materials).

In most cases, the numerical simulation reveals two possible static structures, such as the bipolar structure and the radial structure, or the radial structure and the axial structure. depending on the initial guess of the director configuration. Just which one is more stable can decided by comparing their energies.

In case of $\sigma = 0$ and without the electric field, both the concentric structure and the radial structure are stable (Fig. 1, (a) and (b)). The application of a electric field makes them change into the deformed bipolar structure(Fig. 5) and the deformed radial structure (Fig. 3) respectively. Increasing the electric field strength makes the directors in these structures more and more aligned along the electric field direction. Comparison of their energies shows that the radial structure has lower energies.

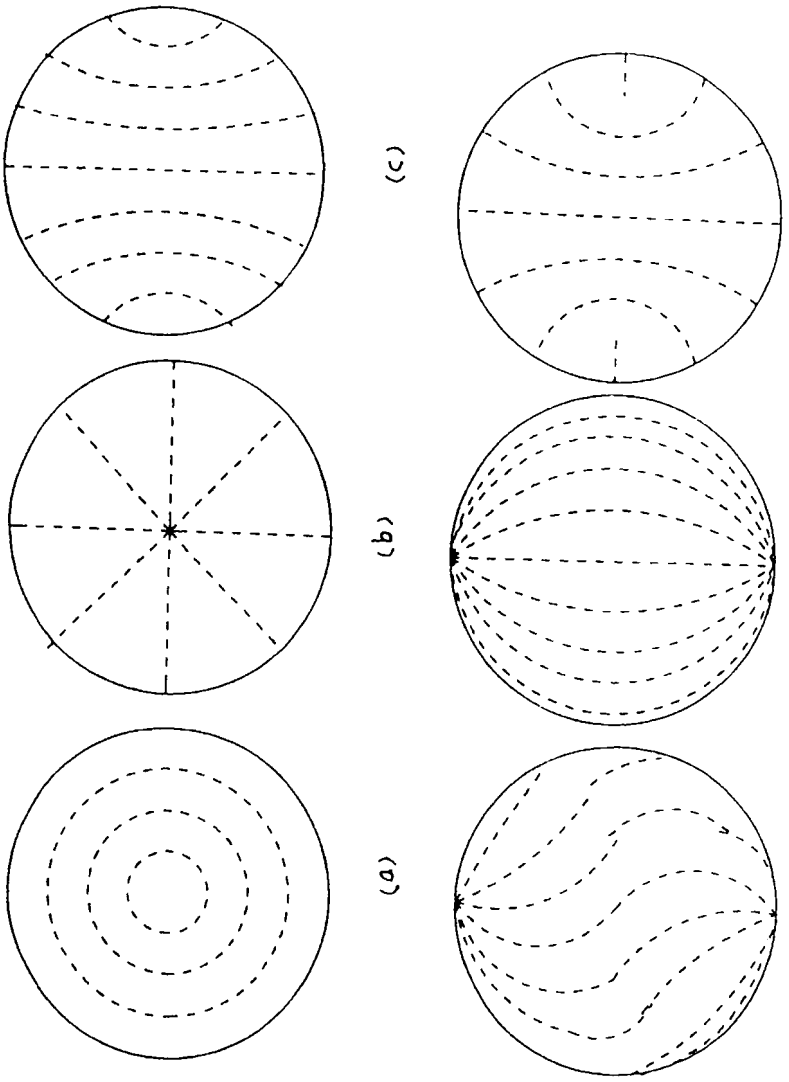

Figure 1: Schematic representation of the most common structures in a nematic droplet: (a) concentric, (b) radial, (c) axial, (d) twisted bipolar, (e) bipolar, (f) axial with a defect line.

For $\sigma \neq 0$, there are two cases:

1. When $\frac{\sigma}{\xi} > 0.1$, both the radial structure and the axial structure are stable. In the radial structure (Fig. 3), usually there is a point defect at the center of the sphere. Under a high electric field, the point defect stretches along the electric field direction until it disappears and the structure becomes the axial one. In the axial structure (Fig. 6-7), the largest deformation occurs along the equator, and a line defect along the equatorial plane appears if the anchoring strength exceeds a certain value (in our case, when $\frac{\sigma}{\xi}$, a line defect occurs, see Fig. 7). In both structures, increasing the anchoring strength makes them more deformed while increasing the electric field makes the molecules more homogeneously aligned along the field direction. Comparison of their energies shows that when σ exceeds certain value (in our case $\sigma = 7$ when $\mu = 0.1$, $\sigma = 6$ when $\mu = 1.0$, $\sigma = 5$ when $\mu > 1.0$) axial structures have lower energy.

2. When $\frac{\sigma}{\xi} > 0.1$, both the radial structure and the axial structure are stable. But when $\mu < 4.0$ the radial structure has lower energy while for $\mu > 4.0$ the bipolar structure has lower energy. For $\sigma = 0$, the bipolar structure with two point defects is an ideal one, while in weak anchoring it deforms into a quasi-bipolar structure without two surface defects (Fig. 5). Up to $\frac{\sigma}{\xi} = 0.1$, this quasi-bipolar structure is nearly homogeneous. With $\frac{\sigma}{\xi} > 0.1$, a transition occurs, it changes into the axial structure. This fact may be useful in practical applications, e. g., certain strength of anchoring may help to reduce the driven voltage of a PDLC film.

The effect of K_{24} in case of $W_0 = 0$ has also been investigated. It shows that for $\frac{K_{24}}{W_0} >> 1.0$ both the radial structure and the bipolar structure are stable, with the radial structure at lower energy. This result means that when K_{24} is relatively large the droplet configuration favors homeotropic anchoring. The effect of variation of K_{24} while keeping $W_0 = 0$ and μ at 10.0, 20.0 respectively has also been investigated. The result shows that the variation of K_{24} practically has no significant effect.

Results on the simulation of optical patterns of various droplet structures under polarized microscope are illustrated in Fig. 2-7 together with their corresponding droplet structures. The viewing direction is along the electric field direction. All simulation are based on the assumption

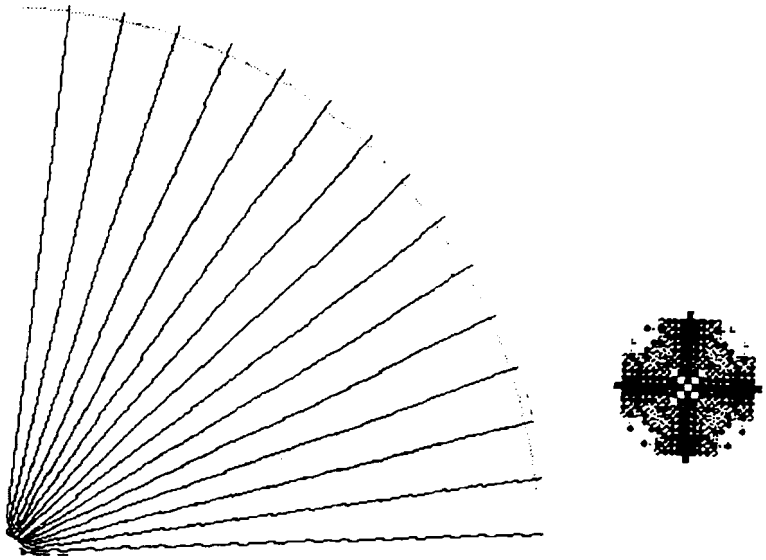

Figure 2: The radial structure (only one quadrant is shown) and it's optical pattern (d/λ = 28.0, n_o = 1.5, n_e = 1.7, d is the diameter of the droplet). μ = 0.0, σ = 5.0.

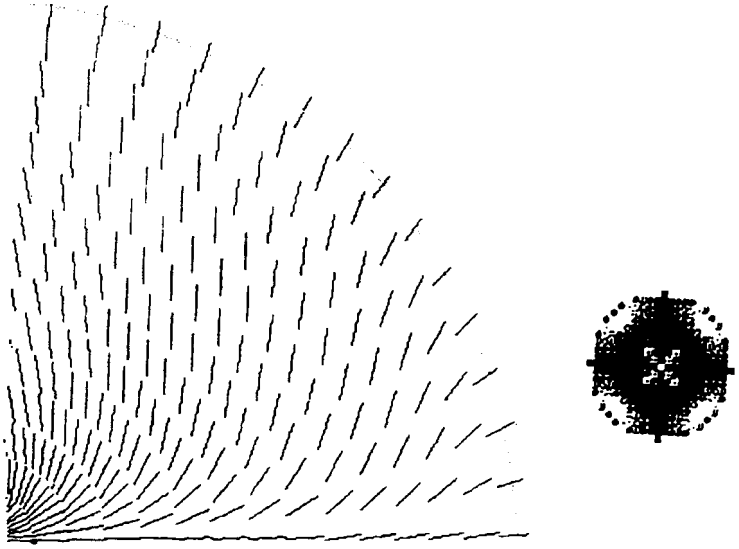

Figure 3: The radial structure (only one quadrant is shown) and it's optical pattern(d/λ = 28.0, n_o = 1.5, n_e = 1.7, d is the diameter of the droplet). μ = 100.0, σ = 10.0.

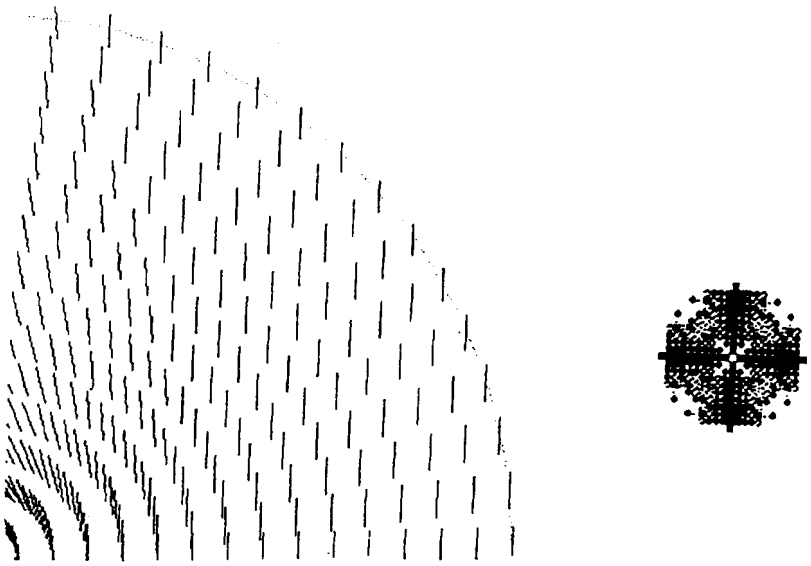

Figure 4: The nearly uiform stucture (only one quadrant is shown) and it's optical pattern(d/λ = 28.0, n_o = 1.5, n_e = 1.7, d is the diameter of the droplet). μ = 100.0, σ = 0.0.

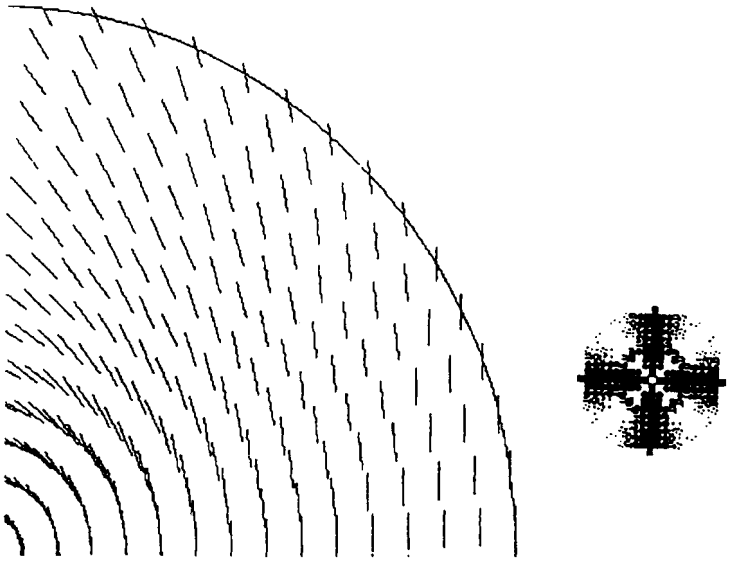

Figure 5: The nearly bipolar structure (only one quadrant is shown) and it's optical pattern(d/λ = 28.0, n_o = 1.5, n_e = 1.7, d is the diameter of the droplet). μ = 5.0, σ = 0.0.

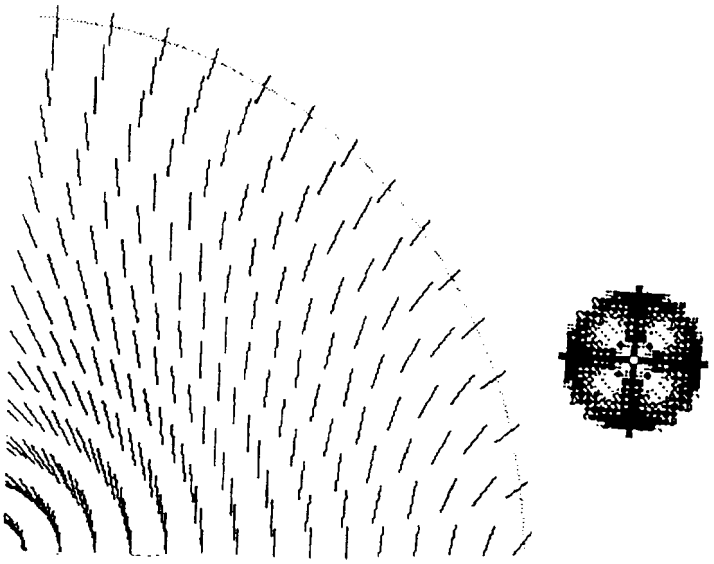

Figure 6: The axial structure (only one quadrant is shown) and it's optical pattern ($d/\lambda = 28.0$, $n_o = 1.5$, $n_e = 1.7$, d is the diameter of the droplet). $\mu = 20.0$, $\sigma = 5.0$.

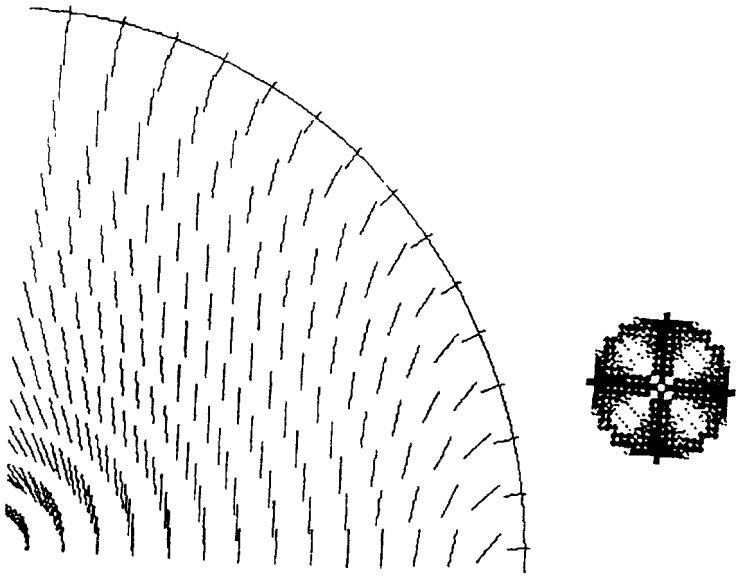

Figure 7: The axial structure with defect (only one quadrant is shown) and it's optical pattern ($d/\lambda = 28.0$, $n_o = 1.5$, $n_e = 1.7$, d is the diameter of the droplet). $\mu = 100.0$, $\sigma = 100.0$

that the difference between the refractive indices of the liquid crystal material and the polymer matrix is so small that the reflection and the refraction effects are neglected. Only phase shifts of ordinary rays and extraordinary rays are taken into account.

V Summary

We have derived general equations for nematic droplet configurations and have investigated various droplet structure transitions. Our numerical procedure is both efficient and simple. It may be useful on PDLC technology and theoretical investigations in which phase transitions, multi-stable states and hesiteresis play an important role.

VI Acknowledgment

This work was carried out on computers belong to the SUN workstation of Institute of Theoretical Physics.

References

[1] R. J. Ondris-Crawford, G. P. Crawford. S. Žumer, and J. W. Doane,Phys. Rev. Lett.,**70**, 194(1993).

[2] John H. Erdmann, Slobodan Žumer, and J. William Doane, Phys. Rev. Lett., **64**, 1907(1990).

[3] E. Dubois-Violette and O. Parodi, J. Phys. Colloq. **30**, C4-57 (1969).

[4] J.Fergason, SID (Society for Information Display), Int. Symp. Digest Techn. Papers **16**, 68(1985).

[5] Liquid Crystals Today (Newsletter of the International Liquid Crystal Society), Vol.5, No.1, April 1995.

[6] S.Kralj, S. Žumer and D. W. Allender,Phys. Rev. **A 43**, 2943(1991).

[7] R. D. J. Williams, J. Phys. **19**, 3211 (1986).

[8] F. Xu, H.-S. Kitzerow and P. P. Crooker, Phys. Rev. **E 49**, 3061 (1994).

[9] P. Sheng, Phys. Rev. **A 26**, 1610(1982).

[10] J. W. Doane, S. Žumer, D. W. Allender and A. Golemme, Phys. Rev. Lett. **61** 2937(1988).

[11] Wei Huang and G. F. Tuthill, Phys. Rev. **E 49**, 570(1994).